Acta Crystallographica Section D
Biological Crystallography
ISSN 0907-4449

Selenomethionine substitution of orotidine-5′-monophosphate decarboxylase causes a change in crystal contacts and space group

Jens-Christian Navarro Poulsen,[a] Pernille Harris,[a] Kaj Frank Jensen[b] and Sine Larsen[a]*

[a]Centre for Crystallographic Studies, Department of Chemistry, University of Copenhagen, Universitetsparken 5, DK-2100 Copenhagen Ø, Denmark, and [b]Institute of Molecular Biology, University of Copenhagen, Sølvgade 83 H, DK-1307 Copenhagen K, Denmark

Correspondence e-mail: sine@ccs.ki.ku.dk

Received 4 January 2001
Accepted 22 June 2001

PDB References: *E. coli* SeMet ODCase, 1jjk; *E. coli* native ODCase, 1eix.

Orotidine 5′-monophosphate decarboxylase (ODCase) catalyses the decarboxylation of orotidine 5′-monophosphate to uridine 5′-monophosphate, the last step in the *de novo* biosynthesis of uridine 5′-monophosphate. In order to determine the structure of ODCase from *Escherichia coli* by the multi-wavelength anomalous dispersion technique, both native and SeMet-substituted proteins have been produced and purified. During the production of SeMet ODCase, it was observed that SeMet was the only amino acid that it was necessary to add to the defined medium during expression. SeMet-substituted ODCase in complex with the inhibitor 1-(5′-phospho-β-D-ribofuranosyl)barbituric acid crystallizes under similar conditions as the native enzyme. In contrast to the native enzyme, where the crystals belong to the orthorhombic space group $P2_12_12_1$, the SeMet-substituted enzyme crystallizes in the monoclinic space group $P2_1$, with a quadrupling of the volume of the asymmetric unit. Despite the drastic difference in symmetry, the overall crystal packing is effectively identical in the two crystal forms. The change in space group appears to originate in differences in the crystal contacts near the SeMet and Met residues. These differences can be rationalized in terms of SeMet's larger size and hydrophobicity.

1. Introduction

Orotidine 5′-phosphate decarboxylase (ODCase; E.C. 4.1.1.23) catalyses the decarboxylation of orotidine 5′-monophosphate (OMP) to uridine 5′-monophosphate (UMP). This reaction is the sixth and final step in the *de novo* biosynthesis of UMP, which is the precursor of all pyrimidine nucleotides in RNA and DNA. ODCase is a monofunctional protein in prokaryotes and fungi, whereas in higher eukaryotes ODCase is part of the bifunctional enzyme UMP synthase, in which ODCase makes up the C-terminal part and orotate phosphoribosyltransferase (E.C. 2.4.2.10) the N-terminal part. The non-enzymatic conversion of OMP to UMP in neutral aqueous solution has been estimated to have a half-life of 78×10^6 years at 298 K (Radzicka & Wolfenden, 1995). The extreme slowness of this reaction has been attributed to the putative carbanion intermediate, which cannot be stabilized by delocalization of the negative charge. Radzicka & Wolfenden (1995) estimated that ODCase enhances the reaction rate by a factor of 10^{17}; this is achieved without use of cofactors such as thiamine, pyridoxal, pyruvoyl or metal ions which are used by other decarboxylating enzymes (O'Leary, 1992). As a first step towards obtaining a better understanding of the function of ODCase, we set out to determine the three-dimensional structure of ODCase from *E. coli*. To use the

multi-wavelength anomalous dispersion technique (MAD) around the anomalous signal from selenium (Hendrickson *et al.*, 1990) for structure determination, both native and selenomethionine (SeMet) substituted ODCase have been produced and purified. Both the native and the SeMet-substituted enzyme were crystallized in complex with the presumed transition-state analogue 1-(5′-phospho-β-D-ribofuranosyl)barbituric acid (BMP), which shows a K_i of 8.8×10^{-12} *M* at pH 6.0. The subsequent structure determination using SeMet-substituted crystals turned out to be a challenge, as it involves the localization of 128 Se atoms in the asymmetric unit, which is four times that of the native enzyme. Neglecting the quadrupling of the unit cell, the problem was reduced to 32 Se atoms in the asymmetric unit by processing the data using the symmetry and unit cell observed in the native crystals (Harris *et al.*, 2000). Knowing the structure of the native protein, we have been able to determine the four-fold larger SeMet-substituted structure by molecular replacement. In this work, we present these results and make a comparison of the SeMet and native structures in order to describe the similarities and especially the differences that have led to the unexpected difference in the space-group symmetry.

2. Materials and methods

2.1. Construction of the expression system

The expression vector pLFF8 has previously been shown to carry the *E. coli pyrF-orfF* operon which encodes ODCase and a small protein of unknown function (Turnbough *et al.*, 1987). *pyrF* is transcribed from the PA1/O4/O3 promoter which is under control of the *lacI* repressor (Deutschle *et al.*, 1986). To construct the plasmid pLFF8, the *pyrF-orfF* region was copied as a PCR fragment from DNA of the previously isolated transducing λ*ppyrF* phage (Jensen *et al.*, 1984). The PCR reaction was performed using Vent polymerase and the two flanking primers 5′-AAGGGATCCATAAGAAGG-TCTGGTCATGACGTTAACTG and 5′-AGGAAGCTTTT-TATGTTAACCGCCTGCGAG, carrying cleavage sites for the restriction endonucleases *Bam*HI and *Hin*dIII, respectively. The resulting PCR fragment was cut with the two restriction enzymes, ligated into plasmid pUHE23-2 previously cut with the same enzymes and treated with alkaline phosphatase to prevent self-ligation. The ligation mixture was transformed into the *E. coli* strain NF1830 (MC4100 *recA1*/F′*lacI*^{q1} *lacZ*::Tn*5*; Bonekamp *et al.*, 1984) and the vast majority of colonies that appeared on an LB-broth agar plate containing ampicillin (100 μg ml^{-1}) carried plasmids similar to the chosen pLFF8. The nucleotide sequence of the cloned *Bam*HI–*Hin*dIII insert was controlled by sequencing and no deviation from the published sequence (Turnbough *et al.*, 1987) was observed.

The *E. coli* K12 strain SØ6735 (*metA, rph-1, recA56 srlC300*::Tn*10* [F′*lacI*^{q1} *lacZ*::Tn*5*]) is a derivative of DL41 (*E. coli K12 metA, rph-1*), which has previously been used for preparation of SeMet-substituted proteins (Hendrickson *et al.*, 1990). The *recA56* mutation prevents homologous recombination between plasmid and the bacterial chromosome. The *recA56* mutation was introduced into strain DL41 by co-transduction with the closely linked *srlC300*::Tn*10* marker selecting resistance to kanamycin. Subsequently, the *F′lacI*^{q1} *lacZ*::Tn*5* episome was introduced by mating with strain NF1830, selecting resistance to tetracycline on glucose-salt minimal agar plates containing Met, as described previously (Bonekamp *et al.*, 1984).

2.2. Expression

The native ODCase was purified from *E. coli* strain NF1830 transformed with pLFF8. The cells were grown with vigorous aeration at 310 K in LB broth (Miller, 1972) containing 100 μg ml^{-1} ampicillin. Protein synthesis was induced by addition of 0.5 m*M* isopropyl-β-D-thiogalactoside (IPTG) when the OD_{436} of the culture was 0.5. The culture was grown to stationary phase overnight. Cells were harvested by centrifugation and the cell pellet was stored frozen at 253 K until use.

SeMet-substituted ODCase was purified from *E. coli* strain SØ6735 transformed with pLFF8. The starter culture was grown with vigorous aeration at 310 K in the (A+B) medium of Clark & Maaløe (1967) supplemented with 0.5% glucose, 4 μg ml^{-1} thiamine, 40 μg ml^{-1} uracil, 100 μg ml^{-1} ampicillin and 50 μg ml^{-1} L-Met. The cells were harvested by centrifugation in the exponential growth phase and resuspended to an OD_{436} of 0.1 in prewarmed medium of the same type, but with 100 μg ml^{-1} DL-SeMet replacing L-Met. Expression of the cloned genes was induced at OD_{436} = 0.5 and continued as described above.

LeMaster medium containing 17 amino acids (not Met) has been recommended for the growth of DL 41 (John Horton, Document Release 2.0). As DL 41 is only auxotrophic for Met, we investigated the need to add all these amino acids in the production of SeMet-substituted ODCase. Four different growth conditions were compared. SØ6735 was grown at 310 K in (A+B) minimal medium with supplement as above and four different combinations of 50 μg ml^{-1} L-Met, 100 μg ml^{-1} DL-SeMet and a 19 amino-acid mix consisting of all amino acids except Met (each amino acid at 0.2 mg ml^{-1}). The resulting growth curves of these experiments are seen in Fig. 1. All four cultures were induced with IPTG (0.5 m*M*) when OD_{436} = 0.8. From Fig. 1 it can be seen that there is great variation between the growth rates of the cultures, but the cell density reaches the same level overnight. ODCase activity in the cell lysates was measured and the four lysates showed comparable ODCase activities (Table 1). In our subsequent production of SeMet-substituted ODCase it was therefore chosen not to include other amino acids in the defined medium.

2.3. Purification and activity measurements

The native ODCase from *E. coli* was purified following a six-step procedure. All columns were equilibrated with buffer devoid of salt before use. 20.0 g of cells were resuspended in

80 ml 68 m*M* Tris pH 7.8 and disrupted by ultrasonic treatment on ice for 30 × 1 min. The extract was centrifuged at 16 000*g* for 30 min at 277 K. Streptomycin sulfate was added to the supernatant to a final concentration of 1% and the solution was left at 277 K for 1 h. The slurry was centrifuged at 16 000*g* for 30 min at 277 K and the supernatant was dialysed overnight against 2 × 1 l 20 m*M* Tris pH 7.8, 5 m*M* mercaptoethanol. The dialysed supernatant was centrifuged as above and then applied to a DEAE-52 column (100 ml, Whatman). ODCase was eluted from the column by a 500 ml linear gradient of NaCl from 0 to 1.5 *M* in 20 m*M* Tris pH 7.8. Selected fractions having ODCase activity were pooled and UMP was added to 5 m*M*, after which the pool was subjected to heat treatment at 339 K for 7.5 min. The heat-treated pool was centrifuged at 10 000*g* for 30 min at 277 K and the supernatant was applied directly to a Matrix Red-A column (40 ml, BioRad). ODCase was eluted from the column with a 240 ml linear gradient of KCl from 0 to 1.2 *M* KCl in 20 m*M* Tris pH 7.8. Selected fractions with ODCase activity were pooled and concentrated in a Centriprep 10 device. The concentrated sample was then applied to a Sephadex 100 column (300 ml, Pharmacia) using a 20 m*M* Tris pH 7.8 buffer containing 5 m*M* mercaptoethanol. Selected fractions with ODCase activity were pooled and applied to an Uno-Q6 column (5 ml, BioRad). ODCase was eluted with a 50 ml linear gradient of NaCl from 0 to 0.2 *M* NaCl. The purest fractions with ODCase activity were pooled and concentrated in a Centriprep 10 device to a protein concentration of about 15 mg ml^{-1} and then dialysed twice against 20 m*M* Tris pH 7.8, 1 m*M* DTT. Sodium azide was added to the dialysed pool to 0.01% and this protein stock solution was stored as 200 µl aliquots at 277 K. The concentration of purified ODCase was estimated using an extinction coefficient of 9650 M^{-1} cm^{-1} at 280 nm, which was calculated from the amino-acid composition according to Gill & von Hippel (1989). ODCase activity was measured by following the conversion of OMP to UMP using the absorbance change at 290 nm ($\Delta\varepsilon = 1900\ M^{-1}\ \mathrm{cm}^{-1}$) (Turnbough *et al.*, 1987). The yield was 15 mg of purified native ODCase per litre of medium. The specific activity of the native ODCase was estimated to be 113 units mg^{-1}. The SeMet-substituted ODCase was purified by a similar procedure as the native ODCase, but the heat treatment was omitted. The SeMet-substituted ODCase was stored as 200 µl aliquots at 253 K. The yield of SeMet ODCase was similar to that of the native protein and the specific activity of SeMet-substituted ODCase was measured to be 98 units mg^{-1}. Amino-acid analysis verified the substitution of Met by SeMet, measuring eight SeMet residues per monomer of ODCase. Additionally, we performed energy-dispersive X-ray fluorescence (Laursen, 1985) to test for metal ions in the protein. The protein solution was dialysed against a metal-free buffer and prepared as described elsewhere (Bukrinsky, 1998). The measurement was performed with Mo $K\alpha$ radiation and no metal ions were detected. In the SeMet-substituted protein we found eight Se atoms (SeMet) for every three S atoms (Cys), as expected from the deduced amino-acid sequence of the *pyrF* gene. These results were in agreement with the values from the amino-acid analysis and show complete substitution of all Met residues by SeMet residues.

Table 1
Comparison of ODCase activity in cell lysate.

Growth condition	Units ml^{-1} OD_{43}^{-1}
L-Met + 19 amino-acid mix	0.66
L-Met	0.29
DL-SeMet + 19 amino-acid mix	0.35
DL-SeMet	0.21

2.4. Crystallization of ODCase complexed with BMP

The ODCase from yeast has previously been successfully cocrystallized with the high-affinity inhibitor BMP (Bell *et al.*, 1991); we also attempted to obtain crystals of the ODCase from *E. coli* complexed with BMP. BMP was added to the protein solution in a fivefold molar excess just prior to setup of the crystallization experiments. Crystallization conditions

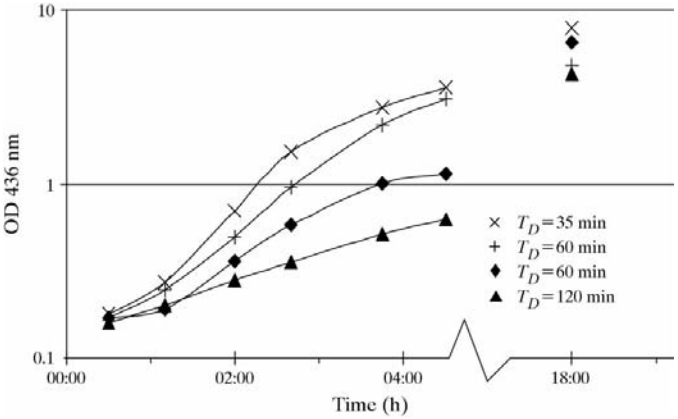

Figure 1
Growth curves of SØ6735 transformed with pLFF8. Defined media added are ×, L-Met + 19 amino-acid mix; +, L-Met; filled diamond, DL-SeMet + 19 amino-acid mix; triangle, DL-SeMet. TD is the doubling time of the culture.

Figure 2
Pseudo-orthorhombic crystals of the SeMet-substituted ODCase complexed with BMP; typical dimensions are 30 × 30 × >500 µm.

were achieved at room temperature by vapour diffusion from hanging drops consisting of 2 µl protein solution and 2 µl reservoir solution. The footprint solubility screen (Stura *et al.*, 1992) was used to judge the solubility of the ODCase–BMP complex. Using Crystal Screens 1 and 2 from Hampton Research (Cudney *et al.*, 1994; Jancarik & Kim, 1991) we screened for crystallization conditions. The optimized conditions for growing crystals of the ODCase–BMP complex were ~291 K, hanging drop, 4 µl protein solution at 6.0 mg ml^{-1} (2.2 AU_{280}) + 4 µl reservoir solution (500 µl 28% PEG 8000, 0.2 *M* $MgCl_2$, 0.1 *M* MES pH 7.0). The reservoir solution was overlaid with 500 µl oil solution made of 90% paraffin oil and 10% silicone oil to reduce the vapour-diffusion rate (Chayen, 1997). Crystals of SeMet-substituted ODCase complexed with BMP used for diffraction experiments are shown in Fig. 2. These were crystallized under slightly different conditions: 291 K, hanging drop, 4 µl protein solution at 6.0 mg ml^{-1} (2.2 AU_{280}) + 2 µl reservoir solution (20% PEG 8000, 0.2 *M* $MgCl_2$, 0.1 *M* MES pH 7.0).

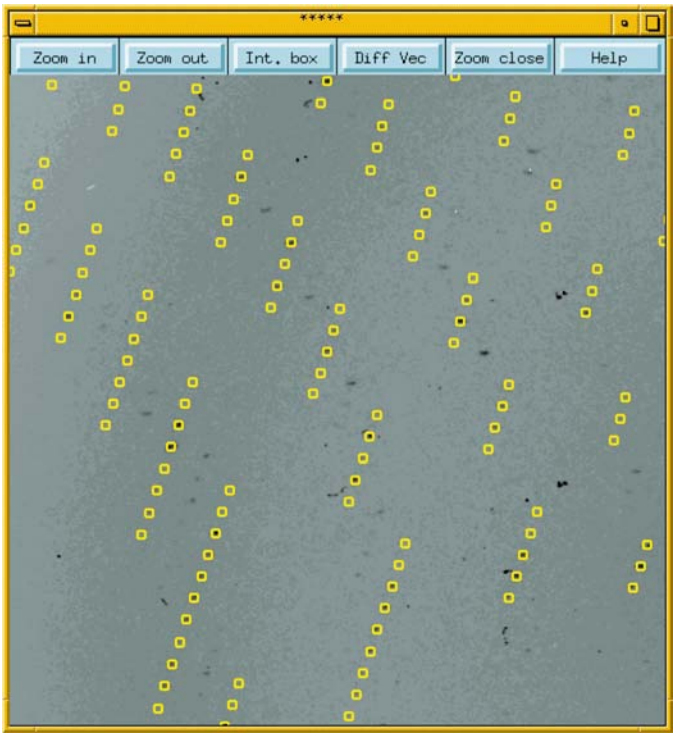

Figure 3
The diffraction pattern from the crystals of the SeMet-substituted ODCase–BMP complex. The circles enclose spots that may be indexed in the small unit cell of the native protein. Spots not enclosed by circles are those giving rise to the unit-cell doubling. The large irregular spots are the so-called zingers.

2.5. Data collection

The crystals of the ODCase–BMP complex were very small and showed very weak diffraction with our in-house R-AXIS II system. The crystals used for data collection were mounted at the synchrotron sites, using 20% glycerol included in the mother liquor as cryoprotectant.

The data from the native crystal were collected at BL I 711 at MAXLAB; a summary of the data collection and the data processing has been reported previously (Harris *et al.*, 2000). It was shown that the diffraction pattern could be indexed in space group $P2_12_12_1$, with unit-cell parameters a = 62, b = 95, c = 145 Å. The MAD data collection on the SeMet-substituted protein complexed with the inhibitor BMP was performed at beamline BM14 at the ESRF using a MAR CCD detector. An exposure time of 3 min on each image was required and unfortunately our images became polluted with so-called zingers, a phenomenon known on synchrotron sources with CCD detectors and long exposure times. To overcome this problem, the data were processed in *DENZO* (Gerwith, 1999), with a very low overload value (10 000 instead of the usual 65 000). In this way, we did not interfere with the rather weak diffraction pattern from the crystal, but managed to remove many zingers from the data.

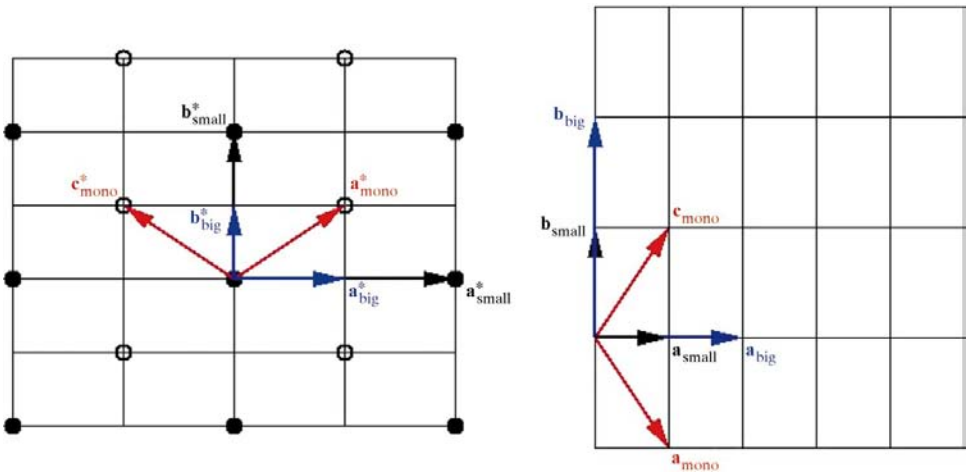

Figure 4
The different cell settings that were considered for the SeMet-substituted crystal form of the ODCase–BMP crystals shown in (*a*) reciprocal and (*b*) direct space. a_{small} and b_{small} correspond to space group $P2_12_12_1$, a_{big} and b_{big} correspond to the unit-cell choice in space group $C222_1$ and a_{mono} and c_{mono} to the monoclinic unit cell in $P2_1$.

The crystals of the SeMet-substituted protein complexed with BMP show a unit-cell doubling in the *ab* plane as briefly described in Harris *et al.* (2000). Fig. 3 illustrates this phenomenon, where circles are lacking around reflections that could not be indexed in the small unit cell corresponding to the native crystals. The extra reflections were systematically weak and should not be mistaken for zingers, which are very strong irregular spots.

All reflections from the SeMet-substituted crystals could be indexed in space group $C222_1$, with unit-cell parameters a = 123.2, b = 195.2, c = 148.9 Å, or alter-

Table 2
Data collection and processing of the SeMet data set.

	$P2_12_12_1$ (pseudo), $P2_1$ and $C222_1$		
X-ray source	BM14, ESRF, Grenoble		
Detector	MAR Research CCD		
Wavelength (Å)			
Peak	0.9787		
Inflection point	0.9789		
Remote	0.8856		
Temperature (K)	105		
Resolution† (Å)	30.0–3.0 (3.16–3.00)		
	$P2_12_12_1$ (pseudo)	$P2_1$	$C222_1$
Unit-cell parameters (Å, °)	a = 61.82 (1) b = 97.68 (21) c = 148.89 (26)	a = 115.5 (2) b = 149.0 (4) c = 115.6 (2) β = 115.3 (1)	a = 123.63 (2) b = 195.35 (41) c = 148.89 (26)
Total No. of reflections			
Peak	55386	109253	111685
Inflection point	55237	109176	112094
Remote	55577	115673	115564
No. of unique reflections			
Peak	18413	60840	35741
Inflection point	18400	60766	35636
Remote	18346	62675	35734
Completeness†			
Peak	98.6 (89.1)	86.5 (55.6)	98.4 (90.3)
Inflection point	98.6 (90.1)	86.4 (55.9)	98.2 (90.2)
Remote	98.4 (90.0)	89.2 (61.2)	98.5 (90.7)
$I/\sigma(I)$†			
Peak	8.9 (3.9)	7.0 (3.1)	7.3 (3.2)
Inflection point	8.6 (3.4)	6.1 (2.5)	7.0 (2.9)
Remote	9.2 (4.1)	7.4 (3.3)	7.6 (3.4)
$R_{\rm merge}$			
Peak	0.108	0.089	0.139
Inflection point	0.114	0.106	0.150
Remote	0.104	0.085	0.134

† Values in parentheses are for the highest resolution shell.

natively in space group $P2_1$, with unit-cell parameters a = 115.5, b = 148.9, c = 115.8 Å, β = 115.4°. The corresponding length and orientation of the axes in direct as well as in reciprocal space are shown in Fig. 4 together with the smaller pseudo-cell. Merging was performed in both space groups $C222_1$ and $P2_1$, with the corresponding data-processing results shown in Table 2. $R_{\rm merge}$ is significantly lower (0.085–0.106) in $P2_1$ than in $C222_1$ (0.134–0.150). It is not possible to transform from space group $P2_12_12_1$ to space group $C222_1$ with a simultaneous doubling of a and b. There is no problem, however, in going from space group $P2_12_12_1$ to space group $P2_1$, as this latter is a subgroup of $P2_12_12_1$ when the axes are oriented as shown in Fig. 4.

The change in space group between the native and the SeMet-substituted ODCase–BMP is associated with a quadrupling of the volume of the asymmetric unit. With a solvent content of 38% the asymmetric unit could therefore contain as many as 8 × 16 = 128 selenium sites (16 SeMet in each dimer). Considering the quality of the data, we realised that we might encounter severe problems searching for this many sites. As has been described, we were able to solve the native structure (Harris *et al.*, 2000; PDB entry 1eix) simply by ignoring the change in cell and symmetry between the native and the

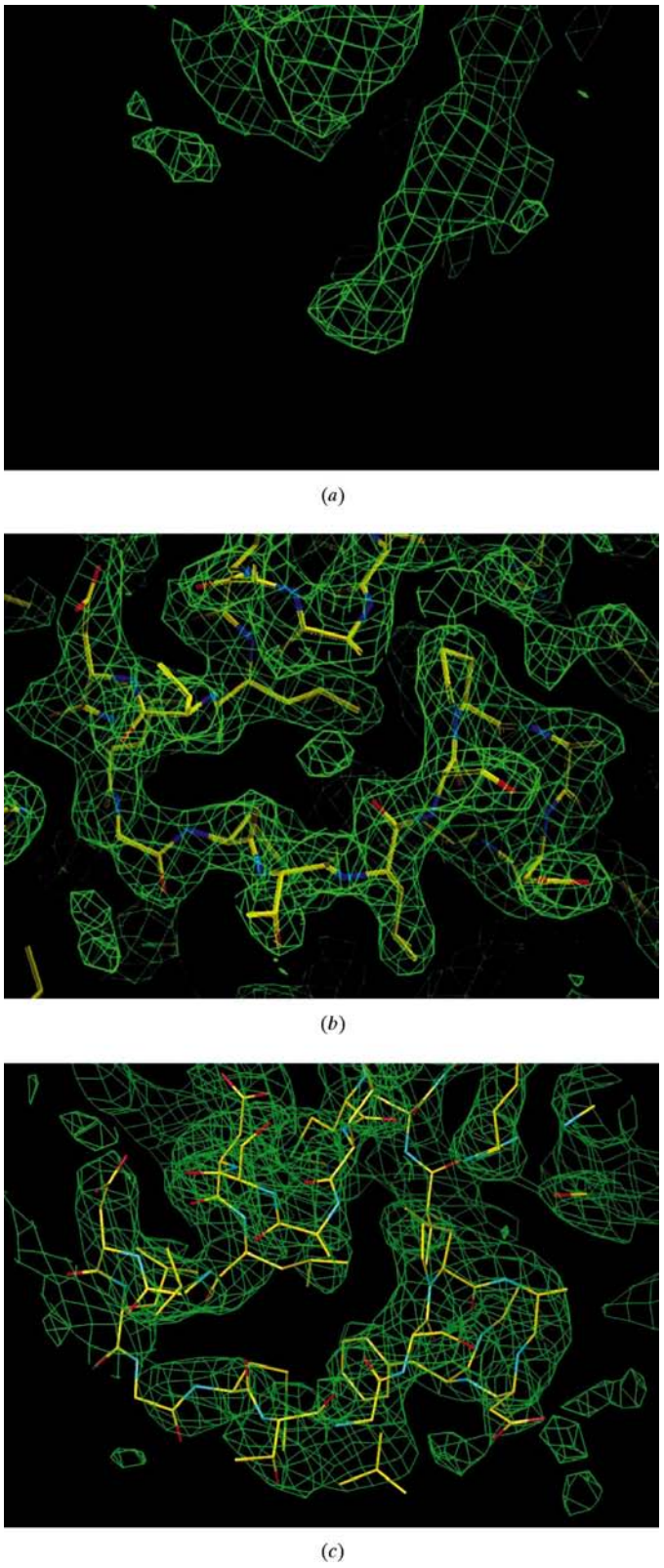

Figure 5
The σ_A-weighted $2F_o - F_c$ maps (contoured to 1σ) in the region of residues 135–150. (*a*) is the map from the SeMet-substituted crystals where the data have been processed in $P2_12_12_1$. (*b*) is the final map of the refinement of the native structure. (*c*) is the final map from the refinement of the SeMet-substituted structure in space group $P2_1$. The figures were produced with *TURBO-FRODO* (Roussel & Cambillau, 1992).

Table 3
Merging of the three SeMet data sets.

Total No. of reflections	333946
No. of unique reflections	64921
Resolution (Å)	30.00–3.00 (3.16–3.00)
Completeness (%)	92.3 (93.7)
$R_{\rm merge}$	0.140 (0.315)
f' average for the three data sets	−6.6

Table 4
Refinement statistics of the preliminary refinement of the SeMet data sets.

Resolution range	30.0–3.0
No. of reflections	61607
No. of atoms	
Protein	1750
Ligand	22
R.m.s.d. (bond lengths) (Å)	0.008
R.m.s.d. (bond angles) (°)	1.431
R	0.342
$R_{\rm free}$	0.349

SeMet-substituted crystals. The data from the SeMet-substituted crystals were processed in space group $P2_12_12_1$, with unit-cell parameters a = 61.81, b = 97.67, c = 148.89 Å, hence neglecting all the systematically weak reflections shown in Fig. 3. The results from the data processing in this space group are shown in Table 2.

3. Structure determination and refinement

The positions of the 28 of 32 Se atoms were determined using the program *SOLVE* (Terwilliger & Berendzen, 1999), where we used the data processed in space group $P2_12_12_1$. Based on the phases from the Se atoms (still using the space group $P2_12_12_1$) a map was calculated to 3.0 Å and about 2/3 of the structure could be built in *TURBO* (Roussel & Cambillau, 1992) and refined in *CNS* (Brunger *et al.*, 1998). This included residues 15–55, 57–135 and 150–239, but parts of the structure were invisible (see Fig. 5*a*). When the refinement was continued against the native data (where $P2_12_12_1$ is the true symmetry) the missing regions of the electron density clearly appeared (as seen in Fig. 5*b*) and the model was corrected and completed. In the final model, residues 12–242 were included (subunit *C* also included residue 243), indicating that the N-terminus and the last few residues of the C-terminus are disordered. The final refinement statistics are given in Table 2 of Harris *et al.* (2000), with an R factor of 0.217 and an $R_{\rm free}$ of 0.261. The disordering of the N-terminus is in agreement with the fact that the first 13 amino acids in the N-terminal part of ODCase are unimportant for enzymatic activity (Jensen *et al.*, 1984).

The SeMet data set had to be refined with 16 molecules in the asymmetric unit in space group $P2_1$. The SeMet data were collected under the assumption that the symmetry was orthorhombic and the data therefore suffered from low completeness and low redundancy. To improve this, we decided to merge all three MAD data sets (also merging the Bijvoet pairs) and adjust f' to the average value of the three. The merging statistics from this process are shown in Table 3. The positions of the 16 molecules were found using the program *AMoRe* (Navaza & Saludjian, 1997) with a very clear solution of correlation 0.751. Rigid-body refinement in *CNS* (Brunger *et al.*, 1998) reduced the R factor to 0.361 and $R_{\rm free}$ to 0.376. It turned out to be very difficult to improve the model purely by refinement, but obvious mistakes were corrected according to the map and several cycles of minimization and B-factor refinement were performed. The R factor was reduced to 0.34 using strict NCS. Given that the native structure was already determined to a resolution of 2.5 Å and that the data from the SeMet crystals extended only to 3.0 Å with half of the reflections systematically weak, it would (if at all possible) require significant efforts to complete the refinement. The relatively high R factors are not associated with any bias in the electron-density maps, which are easily interpretable as can be seen from Fig. 5(*c*). Therefore, we decided not to progress any further with the refinement. The refinement statistics, although preliminary, are shown in Table 4. In Fig. 6, the monoclinic $P2_1$ cell is shown as well as the orthorhombic $P2_12_12_1$ unit cell.

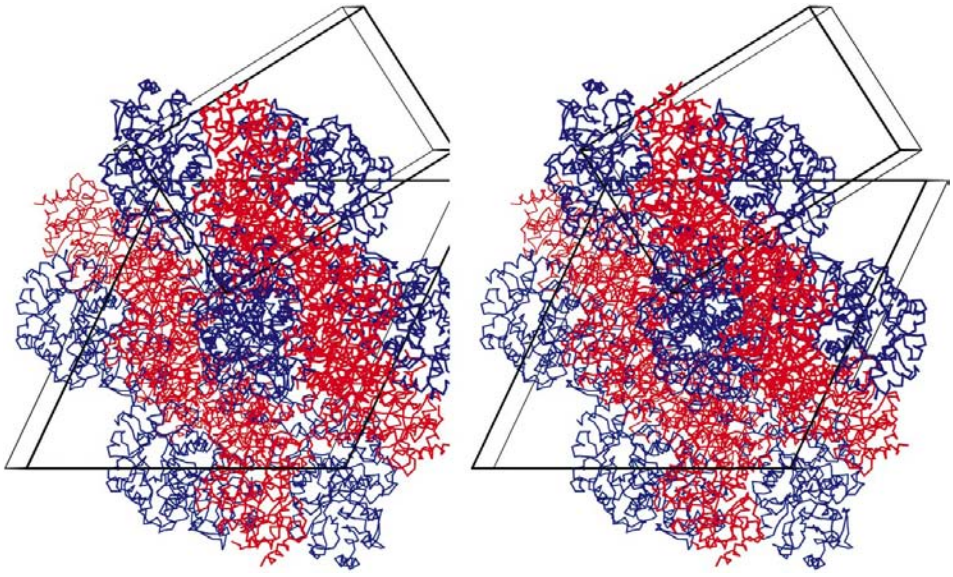

Figure 6
A *MOLSCRIPT* (Kraulis, 1991) stereoview of the crystal packing in the monoclinic $P2_1$ crystal form, viewed down the *b* axis. The unit cell is shown, together with the pseudo-orthorhombic $P2_12_12_1$ cell. The C^α traces of the molecules are shown.

4. Differences between the native and the SeMet-subsitituted crystals

It was pointed out by Smith & Thompson (1998) that the small effects of substituting Met with the larger and more hydrophobic SeMet will be both on the solubility and the stability of the protein. Also, in rare cases it may affect the structure or the crystal packing. We therefore looked for the origin of the difference in symmetry between the native and the SeMet-substituted crystals after having refined the native crystal form.

We have particularly looked for differences in the vicinity of the Met (SeMet) residues. Around Met49, Met106, Met107, Met133, Met205 and Met218 there are no noteworthy differences between the two structures except that the interatomic distances tend to be slightly larger around Se than around S. However, around Met95 and Met143 we do observe some changes in the intramolecular contacts. Because SeMet is more hydrophobic than Met, it will stack with aromatic rings if possible. It may be seen from Figs. 7(*a*) and 7(*b*) that SeMet95 interacts with Phe69 while Met95 does not. As may also be seen from Figs. 7(*c*) and 7(*d*), SeMet143 also interacts more strongly with Tyr150 than does Met143. However, the most pronounced change around this residue is the movement of the backbone, probably because of the larger radius of Se.

When we initially solved the structure and the SeMet data were processed in $P2_12_12_1$, only part of the molecules could be traced. The unresolved parts, which were the N- and

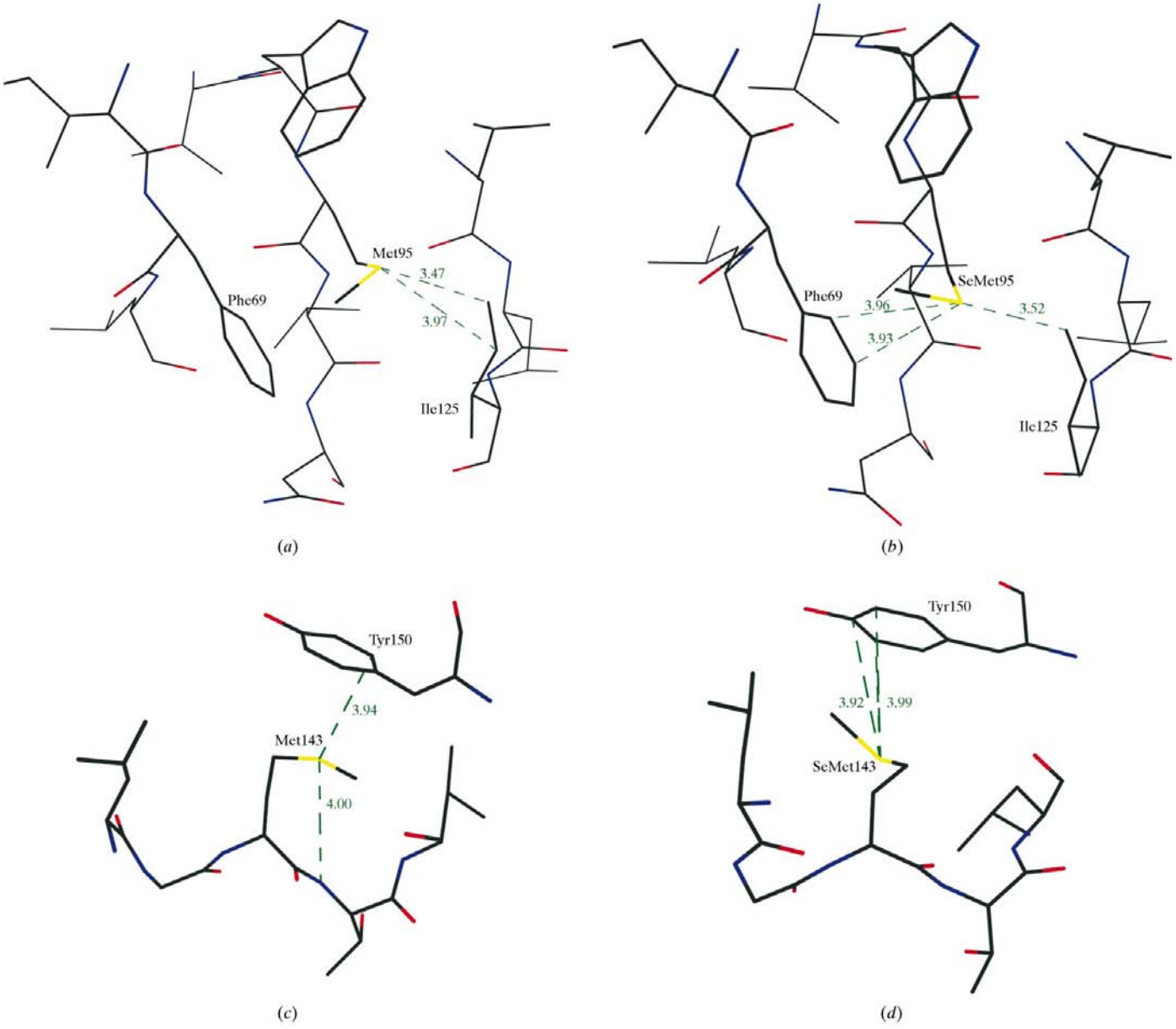

Figure 7
The surroundings of (*a*) Met95 and (*b*) SeMet95 and the surroundings of (*c*) Met143 and (*d*) SeMet143. The figures were produced with *TURBO-FRODO* (Roussel & Cambillau, 1992).

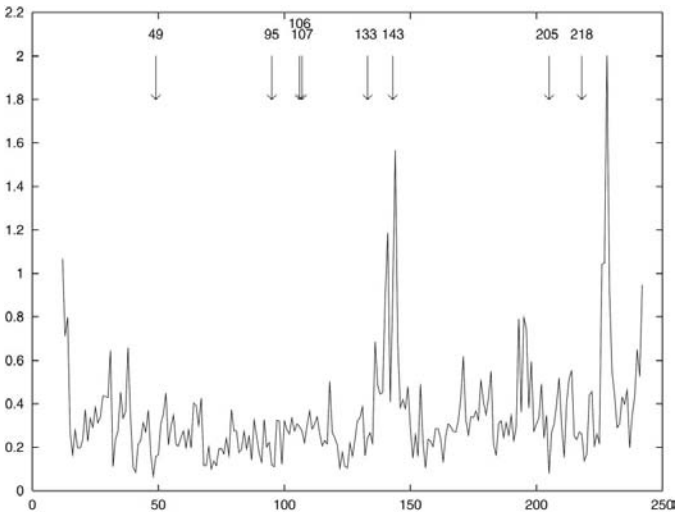

Figure 8
R.m.s. differences of the main chain between the *A* subunit of the native structure and the SeMet-substituted structure calculated with *CNS* (Brunger *et al.*, 1998). The arrows show the positions of the eight methionine residues.

C-termini, the helix 54–66 and residues 135–150, are all at the surface of the dimer. A structural alignment of the *A* subunit of the native and the SeMet-substituted protein was performed; the r.m.s. differences are shown in Fig. 8. The largest deviations in the backbone are seen around residues 143, 200 and 228. All three residues lie in loop regions. Only the loop around residue 143 is in close proximity to Met133 and Met143, which have also been indicated in Fig. 8.

Finally, we performed an analysis of the residues involved in the crystal packing of the two different crystals using the *CCP*4 program *contacts* (Collaborative Computational Project, Number 4, 1994). Here we saw many similarities, but clear differences were also observed. Residues Glu134, Asp140 and Arg153 are involved in intermolecular hydrogen bonds in the native crystal form, but not in the SeMet crystal form. This is compensated for in the SeMet crystal, which uses residues Asp194, Ser196, Pro223, Ser227 and Asp229 to make intermolecular hydrogen bonds. All these residues are near regions that show a large r.m.s. difference between the two structures (see Fig. 8). This indicates that crystal contacts may account for the regions that differ most between the two structures. Furthermore, a region (Glu134, Asp140 and Arg153) which has crystal contacts in the native structure and not in the SeMet-substituted structure is close to two residues, Met133 and Met143. It is probable that the exchange of the latter two with SeMet makes it less favourable for the loop (residues 135–150) to make intermolecular contacts and other regions (Asp194, Ser196, Pro223, Ser227, Asp229) make the contacts instead. This could be the origin of the symmetry change between the two structures.

5. Conclusions

Production of SeMet-substituted protein using the Met auxotrophic DL41 requires only addition of SeMet to the medium and none of the other amino acids. The substitution of Met with SeMet is usually considered completely harmless. However, SeMet is more hydrophobic than Met and selenium has a larger van der Waals radius than sulfur and therefore Met and SeMet may (if possible) make different intra- and intermolecular contacts. The possibility for SeMet of stacking with hydrophobic residues such as aromatic rings has led to minor changes in the ODCase–BMP complex both in the interior and in the loop regions in the enzyme. Some residues which in the native crystals are involved in crystal contacts also are in close proximity to two methionines. In the SeMet-substituted protein, these residues are apparently not able to make the same crystal contacts and other residues must therefore substitute. This means that different residues become involved in the crystal contacts, hence the change in symmetry. It should be emphasized that the packing in the two crystals is essentially the same.

This work has been supported financially by the Danish National Research Foundation. We would like to thank Professor Wayne Hendricksson for providing the *E. coli* strain DL 41 and for the beam-time allocations at BM I711, MAXLab and BM14, ESRF. We are grateful to Flemming Hansen and Lise Schack for excellent assistance and in particular Gordon Leonard at BM14, ESRF for help with the MAD experiments.

References

Bell, J. B., Jones, E. & Carter, C. W. Jr (1991). *Proteins Struct. Funct. Genet.* **9**, 143–151.
Bonekamp, F., Clemmemsen. O., Karlström, O. & Jensen, K. F. (1984). *EMBO J.* **3**, 2857–2861.
Brunger, A. T., Adams, P. D., Clore, G. M., Delano, W. L., Gros, P., Grosse-Kunstleve, R. W., Jiang, J.-S., Kuszewski, J., Nilges, N., Pannu, N. S., Read, R. J., Rice, L. M., Simonson, T. & Warren, G. L. (1998). *Acta Cryst.* D**54**, 905–921.
Bukrinsky, J. (1998). PhD thesis, p. 38, Royal Veterinary and Agricultural University, DK-1871C Frederiksberg, Copenhagen, Denmark.
Chayen, N. E. (1997). *J. Appl. Cryst.* **30**, 198–202.
Clark, D. J. & Maaløe, O. (1967). *J. Mol. Biol.* **23**, 99–112.
Collaborative Computational Project, Number 4 (1994). *Acta Cryst.* D**50**, 760–763.
Cudney, R., Patel, S., Weisgraber, K., Newhouse, Y. & McPherson, A. (1994). *Acta Cryst.* D**50**, 414–423.
Deutschle, U., Kammerer, R., Gentz, R. & Bujard, H. (1986). *EMBO J.* **5**, 2987–2994.
Gerwith, D. (1999). *The HKL Manual: an Oscillation Data Processing Suite for Macromolecular Crystallography.* Yale University, New Haven, USA.
Gill, S. C. & von Hippel, P. H. (1989). *Anal. Biochem.* **182**, 319–326.
Harris, P., Navarro Poulsen, J. C., Jensen, K. F. & Larsen, S. (2000). *Biochemistry*, **39**, 4217–4224.
Hendrickson, W. A., Horton, J. R. & LeMaster, D. M. (1990). *EMBO J.* **9**, 1665–1672.
Jancarik, J & Kim, S.-H. (1991). *J. Appl. Cryst.* **24**, 409–411.
Jensen, K. F., Larsen, J. N., Schack, L. & Sivertsen, S. (1984). *Eur. J. Biochem.* **140**, 343–352.

Kraulis, P. J. (1991). *J. Appl. Cryst.* **24**, 946–950.
Laursen, J. (1985). *Colloquium Spectroscopicum Internationale* XXIV, **1**, 38–39.
Miller, J. H. (1972). *Experiments in Molecular Genetics.* Cold Spring Harbor, NY, USA: Cold Spring Harbor Laboratory Press.
Navaza, J. & Saludjian, P. (1997). *Methods Enzymol.* **276**, 581–594.
O'Leary, M. H. (1992). *The Enzymes*, ch. 6, edited by D. S. Sigman. San Diego: Academic Press.
Radzicka, A. & Wolfenden, R. (1995). *Science*, **267**, 90–93.
Roussel, A. & Cambillau, C. (1992). *TURBO-FRODO biographics and AFMP. Architecture et Fonction des Macromolécules Biologique.*
Smith, J. L. & Thompson, A. (1998). *Structure*, **6**, 815–819.
Stura, E. A., Nemerow, G. R. & Wilson, I. A (1992). *J. Cryst Growth*, **122**, 273–285.
Terwilliger, T. C. & Berendzen, J. (1999). *Acta Cryst.* D**55**, 849–861.
Turnbough, C. L. Jr, Kerr, K. H., Funderburg, W. R., Donahue, J. P. & Powell, F. E. (1987). *J. Biol. Chem.* **262**, 10239–10245.